Ultrasensitive displacement sensing using photonic crystal waveguides

O. Levy[a)]
Department of Solid Mechanics, Materials and Systems, School of Mechanical Engineering, Tel Aviv University, Tel Aviv 69978, Israel

B. Z. Steinberg
Department of Interdisciplinary Studies, School of Electrical Engineering, Tel Aviv University, Tel Aviv 69978, Israel

M. Nathan and A. Boag
Department of Physical Electronics, School of Electrical Engineering, Tel Aviv University, Tel Aviv 69978, Israel

(Received 27 October 2004; accepted 18 January 2005; published online 3 March 2005)

We present an ultrasensitive displacement sensor and sensing technique based on photonic crystal waveguides (PCWG), useful for integration with microelectromechanical system (MEMS) structures. The sensor consists of two PCWGs aligned along a common axis, one mounted on a moving part and the other fixed to a stationary substrate. A gap between the fixed and moving PCWGs creates an intersection with a third, perpendicular PCWG, which has two branches. The intensity exiting each PCWG changes when the suspended PCWG moves in plane relative to the fixed one. The difference in intensities exiting the two perpendicular PCWG branches can be correlated with the relative displacement between the fixed and moving PCWGs. Numerical simulations predict a sensitivity of $\sim 1[\mu m^{-1}]$ using a light source of 9.02 μm. © *2005 American Institute of Physics*. [DOI: 10.1063/1.1880453]

Microelectromechanical system (MEMS) displacement sensors generally rely on the precise measurement of the microdisplacement of a submillimeter flexible component. The displacement may be measured with optical techniques, which can be defined as either intensity or interferometry based.[1] Intensity modulation methods are commonly used, but provide inferior sensitivity relative to interferometry ones. The intensity modulation may be obtained by a relative movement between two optical fiber segments separated by a gap. The overlap area between the two segments determines the amount of energy transferred between the segments.[2] Such devices can provide a sensitivity of $1/90[\mu m^{-1}]$.[3] An increased sensitivity may be obtained by placing a ball lens between the two fiber segments,[2,4] or by creating a ball lens on the fiber edge. Integration of such optical sensors in microoptoelectromechanical systems can be achieved by replacing the optical fibers with dielectric waveguides.

In this letter, we propose a displacement sensor and sensing technique based on photonic crystal (PC) waveguides (PCWG). The sensor includes two coplanar PCWG segments, one fixed and one mobile, aligned along a common axis and separated by a gap, as shown in Fig. 1. In principle, the PC may be any two- or three-dimensional structure possessing a band gap in the frequency domain used for the light signal.[5–7] The fixed PCWG is rigidly connected to a substrate and the mobile PCWG is rigidly connected to a moving part (e.g., a suspended MEMS mass) operative to move in-plane perpendicularly to the common PCWG axis. The gap is essentially an intersecting third PCWG with a left and a right branch (with respect to the input light signal), see Fig. 2. As shown, the left branch extends upward toward a Detector B, while the right branch extends downward toward a Detector C. The sensing is performed by measuring changes in light intensity resulting from the relative displacement between the fixed and moving PCWGs. Energy exiting the fixed PCWG is divided at the intersection, some continuing in the moving section and some split between the left and right branches. The amount of energy exiting each of the moving PCWG and the two branches depends on the displacement.

We now present numerical simulation results in which we analyze the field distribution inside the PC structure, considering that the problem of adiabatic coupling from an external light source is well characterized.[8–10] We use a numerical code based on the multifilament current model[11] to compute the full solution of the propagation/scattering problem, and then to find the energy distribution and intensity exiting each PCWG for different displacements. The simula-

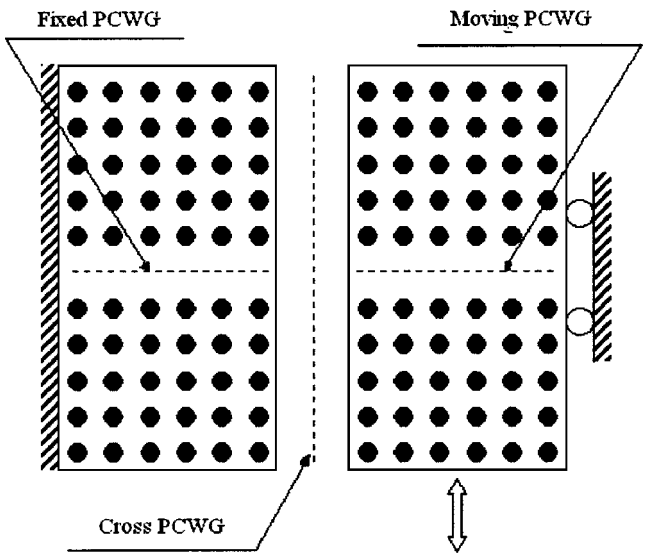

FIG. 1. PC-based displacement sensor layout.

[a)]Electronic mail: oren@eng.tau.ac.il

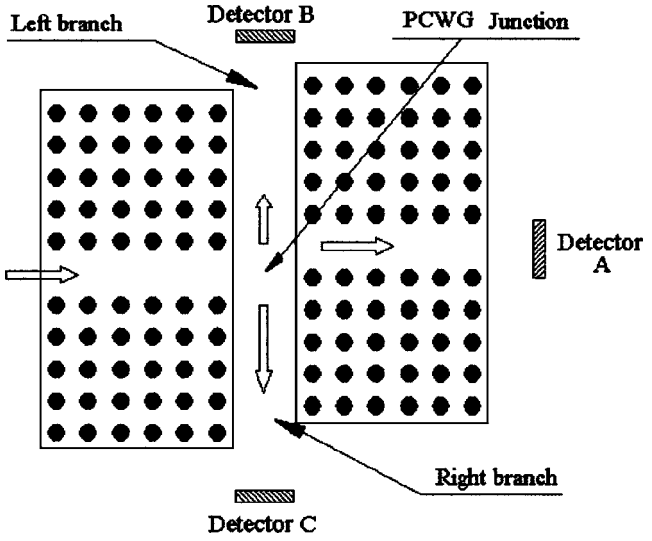

FIG. 2. A schematic description of the PCWG displacement sensor after displacement.

tion is performed on the two-dimensional PC based device of Figs. 1 and 2, which is comprised of round dielectric posts with a diameter of 1.2 μm and a relative dielectric constant $\epsilon=8.41$, separated by air. The posts are positioned on a square periodic lattice with a unit cell of 4 μm by 4 μm. All waveguides are W1-type (i.e., made of one missing row of posts).[12] We use a wavelength of 9.02 μm, which can be generated using a CO_2 laser, and which is within the band gap of this PC structure (for similar structures and band gaps, see, for example, Ref. 7). The numerical code is used to compute the fields for displacements between 0 and 6 μm. Detectors A, B, and C are placed 6 μm away from the respective PCWG output edges. The displacement is correlated with the electric-field intensities, specifically to the difference $\mathbf{I_B}-\mathbf{I_C}$ of the intensities, respectively, reaching Detectors B and C. We first provide a set of simulations results, and then describe the various physical effects that take place in different operation regions.

Figures 3(a) and 3(b), respectively, show the electric-field distribution for displacements of: 0.6 μm and 6 μm. The light pattern and the intensities radiating from the waveguide output edges depend strongly on the displacement. Figure 4 shows the intensities reaching each detector as a function of the displacement. Each graph is normalized to the total intensity exiting the device. That is, $I_A=\mathbf{I_A}/(\mathbf{I_A}+\mathbf{I_B}+\mathbf{I_C})$, where the bold quantities are the actual electric-field intensities (E^2) integrated along the detector surface. Similar relations hold for I_B and I_C. The most interesting quantity is the differential intensity between branches B and C.

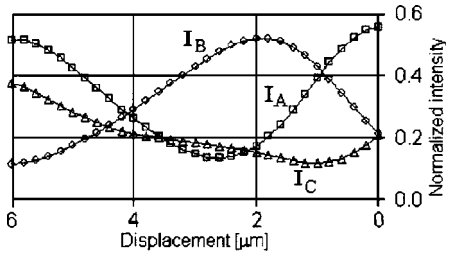

FIG. 4. Normalized intensity as a function of displacement for each detector.

Figure 5 shows the normalized difference $\Delta_{BC}=(\mathbf{I_B}-\mathbf{I_C})/\max[(\mathbf{I_B}-\mathbf{I_C})]$ as a function of the displacement, where $\max[(\mathbf{I_B}-\mathbf{I_C})]$ is the highest value over all displacements. We define sensitivity as the ratio between the normalized difference Δ_{BC} and the corresponding displacement. This ratio is equal to the curve slope in Fig. 5. One sees that there are two displacement ranges in which the sensitivity is high: Region A (0–0.6 μm displacement) with a sensitivity of $\sim 1[\mu m^{-1}]$ and Region B (3–5 μm displacement) with a sensitivity of $\sim 0.4[\mu m^{-1}]$. Region A (relatively small displacements) is the one of interest to us. In this region, small displacements have a profound effect on the waveguide junction (intersection) geometry and, hence, on the scattering effects that take place therein, while the waveguide output terminals are hardly affected by these small displacements. Therefore, $\mathbf{I_B}-\mathbf{I_C}$ and Δ_{BC} reflect differences in the power entering the left and right branches, i.e., are basically determined by the complex scattering and resonance effects that take place at the junction region. For larger displacements, the intersection shape remains relatively unchanged, and the power reaching each detector is essentially a result of the intensity pattern of the field that radiates from the waveguide terminals.

Based on these results, we conclude that there are two important advantages in working with Region A, namely better sensitivity to small displacements and better robustness (for the latter, see below). We note that the sensitivity of $\sim 1[\mu m^{-1}]$ shown above is achieved using a PC structure designed for light signals with a wavelength of 9.02 μm. Similar structures for shorter wavelengths can easily be de-

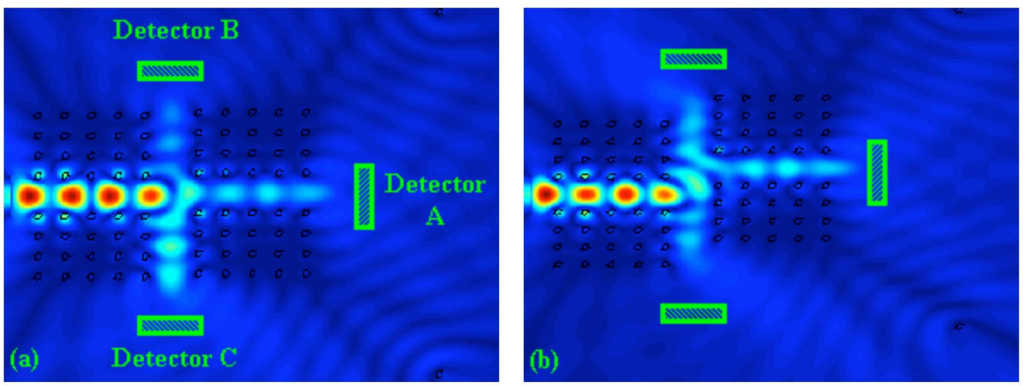

FIG. 3. (Color online) Electric-field distribution in a PCWG sensor after a displacement of: (a) 0.6 μm and (b) 6 μm.

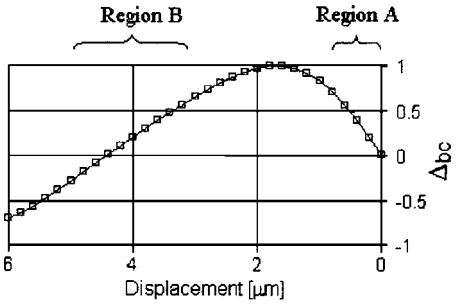

FIG. 5. Normalized intensity difference $\Delta_{BC}=(\mathbf{I_B}-\mathbf{I_C})/\max[(\mathbf{I_B}-\mathbf{I_C})]$ as a function of displacement.

signed by performing a proper geometry downscale. We predict that the sensitivity will increase by a corresponding factor. For example, if the wavelength used is 1.5 μm, the sensitivity is predicted to increase by a factor of 6.

The robustness of such a device in terms of fabrication and dimensional errors is an important factor in actual implementations. We performed simulations that checked the effects of structural disorder on the device sensitivity in three different cases: (1) for detectors misplaced relative to the PCWG edges; (2) for effects of random fabrication errors in the PC structure in the range of ± 0.075 μm; and (3) for changes of the gap between the two PCWGs. In case (1), we checked the device sensitivity starting with the detectors aligned with the PCWG edge (zero distance) and then moved by 2 μm, 4 μm, and 6 μm away of the PCWG edges. The results are shown in Fig. 6. The effect of the detector location on the sensitivity in Region A is very small compared to that in Region B. This is so because the energy reaching Detectors B and C is essentially due to differences in the power entering the left and right branches at the junction. In contrast, in Region B, the energy reaching the detectors is determined by the intensity pattern of the field radiating out of the waveguide terminals.

The fabrication of the suggested PC structure may also involve errors in the location and radius of the posts. We performed several simulations with random errors of ± 0.075 μm (with uniform distribution) in these two parameters. As shown in Fig. 7, the intensity differences $\mathbf{I_B}-\mathbf{I_C}$ for

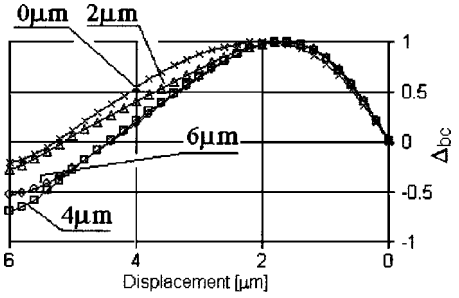

FIG. 6. Normalized intensity difference $\Delta_{BC}=(\mathbf{I_B}-\mathbf{I_C})/\max[(\mathbf{I_B}-\mathbf{I_C})]$ as a function of displacement for several detector positions relative to a PCWG edge.

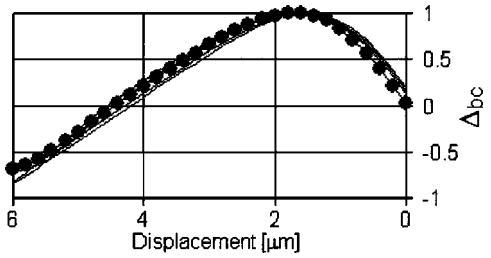

FIG. 7. Normalized intensity difference $\Delta_{BC}=(\mathbf{I_B}-\mathbf{I_C})/\max[(\mathbf{I_B}-\mathbf{I_C})]$ for a sensor with 0.075 μm error in post location and radius. The full circles represent a structure with no errors. Other lines represent various errors.

several different error patterns show similar behavior to that of the error-free structure over the entire displacement range.

The results shown so far were obtained with a waveguide width (and gap size) of 8 μm. We checked the device sensitivity to four other gap sizes: 7.6 μm, 7.8 μm, 8.2 μm, and 8.4 μm. The gap size change in the range of ± 0.4 μm has a negligible effect on the sensitivity, and therefore on the predicted sensor performance.

In summary, we propose a displacement sensor and sensing method based on PCWGs that provide a sensitivity of the order of $\sim 1[\mu\mathrm{m}^{-1}]$ for light with wavelength 9.02 μm. A six-fold increase in sensitivity is predicted for a use of light with wavelength of 1.5 μm and a proper structure downscaling. We note, however, that there are two major factors not considered in the present work which may cause a degradation of these theoretically obtained sensitivity values. As pointed out, our numerical study is based on a two-dimensional model, thus scattering losses in three-dimensional configurations were not handled in a complete and exact way. Furthermore, the dielectric material was assumed to be ideal, i.e., material losses were not considered. Nevertheless, it is expected that these factors will not significantly affect the conclusion that a PCWG-based sensor may provide absolute sub-Angstrom displacement detection. This absolute detection limit will mainly depend on the detectors and associated signal processing.

The authors would like to acknowledge Orli Hershkoviz for help with the simulations.

[1] T. Wang, S. Zheng, and Z. Yang, Sens. Actuators, A **69**, 134 (1998).
[2] H. Golnabi, Rev. Sci. Instrum. **70**, 2875 (1999).
[3] M. Abdelrafik, L. Pierre, M. Jeanine, R. Christine, and F. Pierre, Appl. Opt. **34**, 8014 (1995).
[4] M. Cote and R. R. Shannon, Appl. Opt. **35**, 6179 (1996).
[5] J. D. Joannopoulos, R. D. Meade, and J. N. Winn, *Photonic Crystals: Molding the Flow of Light* (Princeton University Press, Princeton, N.J., 1995).
[6] S. G. Johnson, S. Fan, P. R. Villeneuve, J. D. Joannopoulos, and L. A. Kolodziejski, Phys. Rev. B **60**, 5751 (1999).
[7] E. Centeno, B. Guizal, and D. Felbacq, J. Opt. A, Pure Appl. Opt. **1**, L10 (1999).
[8] Y. Xu, R. K. Lee, and A. Yariv, Opt. Lett. **25**, 755 (2000).
[9] A. Mekis and J. D. Joannopoulos, J. Lightwave Technol. **19**, 861 (2001).
[10] T. D. Happ, M. Kamp, and A. Forchel, Opt. Lett. **26**, 1102 (2001).
[11] Y. Leviatan and A. Boag, IEEE Trans. Antennas Propag. **35**, 1119 (1987).
[12] P. Lalanne and A. Talneau, Opt. Express **10**, 354 (2002).